Top-quark polarization at e^-e^+ colliders

C.-P. Yuan
Institute for Particle Physics, University of California at Santa Cruz, Santa Cruz, California 95064
and Department of Physics and Astronomy, The Johns Hopkins University, Baltimore, Maryland 21218
(Received 21 August 1991)

Once top quarks are found, because they are heavy they will allow many new tests of the standard model and new probes of physics at the 100-GeV scale. In this paper we discuss the polarization of the top quark produced in e^-e^+ collisions for $\sqrt{S}=0.5$ and 1 TeV. The predictions of the top-quark polarization arising from the interactions of QCD, the standard-model electroweak theory, and an electroweak theory with dynamical symmetry breaking is examined.

PACS number(s): 13.88.+e, 13.65.+i, 14.80.Dq

I. INTRODUCTION

Because the standard-model (SM) top quark is much heavier than the other fermions, it is likely that by studying the top quark one can probe for new physics. In a recent work [1], we gave the helicity amplitudes of various top-quark production and decay processes so that one can implement these amplitudes in a Monte Carlo program to study any physical observables. Among these observables the transverse polarization of the top quark was extensively discussed. (In this paper the transverse polarization direction is the one which is perpendicular to the scattering plane, unless otherwise specified.) It was first [2] pointed out by Kane, Pumplin, and Repko that QCD can be tested beyond the tree level by studying the transverse polarization of a heavy quark produced in e^-e^+ or hadron collisions. Recently, it was suggested [3] that one can use the transverse polarization of the top quark to probe the Higgs boson in the standard model. As discussed in Ref. [3], in addition to the Higgs-boson effects, one should also include the gauge-boson contributions, whose leading behavior in the high-energy limit can be well represented by the Goldstone-boson interactions according to the equivalence theorem [4]. However, the work presented in Ref. [3] is incomplete. In contrast with the conclusion in Ref. [3], we show that the degree of transverse polarization of the top quark due to the SM electroweak corrections is smaller than the QCD corrections for a 140-GeV top quark at the NLC (proposed next linear e^-e^+ collider at SLAC, $\sqrt{S}=500$ GeV). This is what we expect because the typical coupling strength of the top quark with the Higgs boson is of $O((1/4\pi)(m_t^2/v^2))$, where m_t is the top-quark mass and v the vacuum expectation value ~ 246 GeV. Therefore, for a 140-GeV top quark, this coupling is small by a factor of 3.9 compared with the typical QCD strength $\alpha_s \sim 0.1$.

In Ref. [1] we showed that the imaginary parts of the form factors $F_1^{L,R}$ and $F_2^{L,R}$ are responsible for the transverse polarization of the top quark produced via the process

$$e^-e^+ \to t\bar{t} \ . \tag{1.1}$$

In terms of these form factors $F_1^{L,R}$ and $F_2^{L,R}$, the helicity amplitudes of the process (1.1) were also given in that reference. Since our primary goal is to obtain the transverse polarization of the top quark, only the imaginary part of these form factors beyond the tree level will be considered. In addition to the QCD and SM electroweak radiative corrections, we also examine a chiral Lagrangian [5], which allows the top quark to have some *nonuniversal* gauge interactions.

This paper is organized as follows. In Sec. II we lay out the procedures of calculating the transverse polarization of the top quark in the $e^-e^+ \to t\bar{t}$ process and justify the validity of using the equivalence theorem (ET) in this application. In Sec. III the contribution to the transverse polarization of the top quark from the QCD corrections at the one-loop level is given. The contribution from the SM electroweak radiative corrections is given in Sec. IV. In Sec. V we discuss the polarization of the top quark in a chiral Lagrangian proposed by Peccei and Zhang in Ref. [5]. Section VI contains some of our conclusions.

II. TRANSVERSE POLARIZATION OF THE TOP QUARK

At tree level the top quark produced in an e^-e^+ collision cannot be transversely polarized because transverse polarization can arise only from the interference of complex helicity-flip and -nonflip amplitudes, while at tree level the amplitudes are relatively real.

Denote the helicity amplitudes of the process (1.1) as $(h_{e^-}, h_{e^+}, h_t, h_{\bar{t}})$, where $h_{e^-}=-,+$, respectively, indicates a left- and a right-handed electron. The degree of transverse polarization ($P_\perp \sin\alpha$) of the top quark perpendicular to the scattering plane for the process (1.1) is defined as [1]

$$P_\perp \sin\alpha = \frac{T_\perp}{G}(\text{color factor}) \ , \tag{2.1}$$

where

$$\begin{aligned} G = &|(+--++)|^2+|(+-+-)|^2+|(+---+)|^2 \\ &+|(+---)|^2+|(-+++)|^2+|(-++-)|^2 \\ &+|(-+-+)|^2+|(-+--)|^2 \end{aligned} \tag{2.2}$$

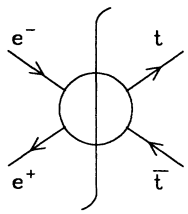

FIG. 1. The blob contains all the one-loop diagrams. The line through the blob indicates to take the imaginary part of the diagrams.

and

$$T_\perp = 2\,\mathrm{Im}[(+-++)^*(+--+) + (+-+-)^*(+---) + (-+++)^*(-+-+) + (-++-)^*(-+--)] . \quad (2.3)$$

The function Im selects the imaginary part of the result. The color factor in Eq. (2.1) for this process is $C_F=\frac{4}{3}$ when considering the contribution to the transverse polarization of the top quark due to the QCD interaction. [A factor of N_C $(=3)$ comes from the Born amplitude squared when calculating G and a factor of $N_C C_F$ comes from the interference term of the Born and the one-loop diagrams when calculating $T_\perp$.] This color factor is 1 when considering the electroweak contributions. Similarly, the degree of transverse polarization ($\overline{P_\perp}\sin\bar{\alpha}$) of the top antiquark for the process (1.1) is

$$\overline{P_\perp}\sin\bar{\alpha}=\frac{\overline{T_\perp}}{G}(\text{color factor}) , \quad (2.4)$$

where

$$\overline{T_\perp} = -2\,\mathrm{Im}[(+-++)^*(+-+-) + (+---)^*(+---) + (-+++)^*(-++-) + (-+-+)^*(-+--)] . \quad (2.5)$$

$\overline{T_\perp}=-T_\perp$ for a *CP*-invariant theory.

The contribution to the transverse polarization of the top quark due to the QCD corrections shall be discussed in the next section. The rest of this section is devoted to the discussion on how to obtain the one-loop radiative corrections, arising from the electroweak interactions, to the transverse polarization of the top quark.

At the one-loop level, the imaginary part of the helicity amplitudes can be obtained by applying the Cutkosky cutting technique [6]. Diagrammatically, it is shown in Fig. 1. The blob contains all the one-loop diagrams. The line through the blob indicates to take the imaginary part of these diagrams. Some of these diagrams are shown in Fig. 2. There the blob represents all the possible tree diagrams. Hence taking the imaginary part of the process (1.1) is equivalent to considering all possible rescattering processes in the *intermediate* state. In this paper we shall only consider the $2\to 2$ rescattering process. For instance, the first diagram in Fig. 2 can be thought of as W^-W^+ pair produced from the e^-e^+ scattering, and then the W^- boson scatters with the W^+ boson to produce the $t\bar{t}$ pair in the final state. Some of the diagrams contained in the first diagram of Fig. 2 are shown in Fig. 3. They can be self-energy, vertex, and box diagrams.

As shown in Fig. 2, this problem can be treated as a *final*-state rescattering process. First of all, we need to find the production rates of

$$\begin{aligned} &e^-e^+\to W^-W^+ , \\ &e^-e^+\to Z^0Z^0 , \\ &e^-e^+\to Z^0H , \\ &e^-e^+\to t\bar{t} , \\ &e^-e^+\to b\bar{b} , \end{aligned} \quad (2.6)$$

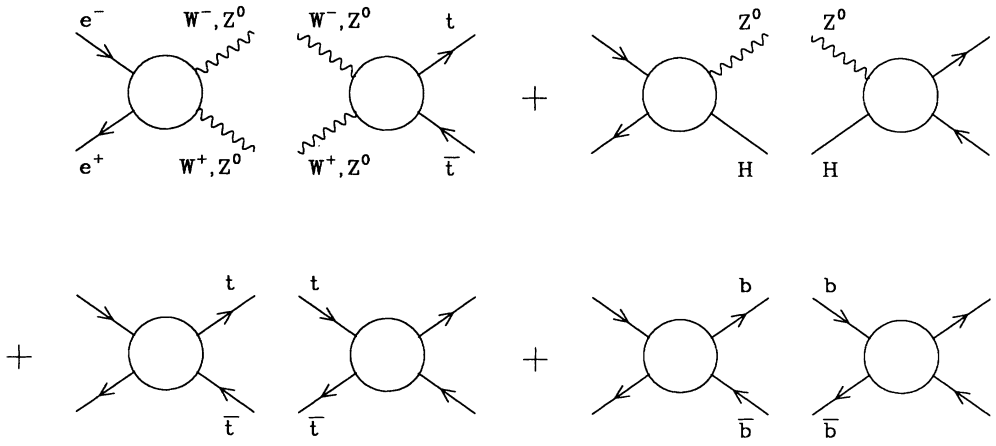

FIG. 2. Some representative diagrams contained in Fig. 1. Here the blob represents all the possible tree diagrams.

etc. The third process does not exist if the Higgs boson is too heavy to be produced on shell. Because of the rules of the Cutkosky cutting technique, all of these final-state partons are on mass shell and can be in any physical polarization states. Then these final-state partons rescatter to produce $t\bar{t}$ as

$$\begin{aligned} &W^-W^+\to t\bar{t}\ ,\\ &Z^0Z^0\to t\bar{t}\ ,\\ &Z^0H\to t\bar{t}\ ,\\ &t\bar{t}\to t\bar{t}\ ,\\ &b\bar{b}\to t\bar{t}\ , \end{aligned} \tag{2.7}$$

etc.

Since we are interested in obtaining the degree of transverse polarization of the top quark for a high-energy e^-e^+ collider, we can simplify the above procedures by applying the ET to obtain the *leading* contributions which are of $O(g^2m_t^2/M_W^2)$. (We note that these leading contributions do not always dominate numerically unless the top quark is extremely heavy [7].) To obtain these leading contributions of the processes (2.7), we use the effective Lagrangian proposed in Ref. [8], which is the SM Lagrangian in the limit of turning off the gauge coupling g, i.e., in the limit of $g\to 0$. In this limit it does not matter whether the SM Lagrangian before taking the limit of $g\to 0$ is in the 't Hooft–Feynman gauge or in the Landau gauge. We therefore consider this effective Lagrangian in the Landau gauge so that the unphysical Higgs bosons are massless to further simplify our calculation. These unphysical Higgs bosons are the Goldstone bosons in the limit of $g\to 0$. The rate of a heavy-top-quark pair production in the first three processes of (2.7) is dominated by the longitudinal $W^\pm$ or Z^0 bosons [9]. Applying the ET, we can obtain the leading behavior of the processes in (2.7) for a heavy top quark by considering the equivalent processes

$$\begin{aligned} &\phi^-\phi^+\to t\bar{t}\ ,\\ &\phi^0\phi^0\to t\bar{t}\ ,\\ &\phi^0H\to t\bar{t}\ ,\\ &t\bar{t}\to t\bar{t}\ ,\\ &b\bar{b}\to t\bar{t}\ . \end{aligned} \tag{2.8}$$

The effective Lagrangian $\mathcal{L}_{\rm eff}$ used to obtain the leading contributions to the transverse polarization of the top quark produced via the processes in (2.8) is

$$\mathcal{L}_{\rm eff}=\mathcal{L}^{\phi}_{\rm kin}+\mathcal{L}^{\phi}_{\rm int}+\mathcal{L}^{f}_{\rm kin}+\mathcal{L}^{f}_{\rm int}\ , \tag{2.9}$$

with

$$\begin{aligned} \mathcal{L}^{\phi}_{\rm kin}&=(\partial_\mu\phi^+)(\partial^\mu\phi^-)+\tfrac{1}{2}(\partial_\mu\phi^0)^2+\tfrac{1}{2}(\partial_\mu H)^2-\tfrac{1}{2}m_H^2H^2\ ,\\ \mathcal{L}^{\phi}_{\rm int}&=\frac{-m_H^2}{8v^2}[H^2+(\phi^0)^2+2\phi^+\phi^-]^2\\ &\quad-\frac{m_H^2}{2v}H[H^2+(\phi^0)^2+2\phi^+\phi^-]\\ &\quad-\tfrac{1}{2}\delta[H^2+(\phi^0)^2+2\phi^+\phi^-+2vH]\ , \end{aligned}$$

$$\begin{aligned} \mathcal{L}^{f}_{\rm kin}&=\bar{t}(i\partial\!\!\!/-m_t)t+\bar{b}(i\partial\!\!\!/-m_b)b+\bar{\nu}_\tau i\partial\!\!\!/\nu_\tau+\bar{\tau}i\partial\!\!\!/\tau\ ,\\ \mathcal{L}^{f}_{\rm int}&=\frac{im_t}{\sqrt{2}v}\phi^+\bar{t}(1-\gamma_5)b-\frac{im_t}{\sqrt{2}v}\phi^-\bar{b}(1+\gamma_5)t\\ &\quad-\frac{im_b}{\sqrt{2}v}\phi^+\bar{t}(1+\gamma_5)b+\frac{im_b}{\sqrt{2}v}\phi^-\bar{b}(1-\gamma_5)t\\ &\quad-\frac{m_t}{v}H\bar{t}t-\frac{im_t}{v}\phi^0\bar{t}\gamma_5t-\frac{m_b}{v}H\bar{b}b+\frac{im_b}{v}\phi^0\bar{b}\gamma_5b\ . \end{aligned} \tag{2.10}$$

In $\mathcal{L}^{f}_{\rm kin}$ and $\mathcal{L}^{f}_{\rm int}$ we include a complete family of ν_τ, τ, t, and b, where the mass of b is kept for completeness, but the mass of τ is set to be zero. $\mathcal{L}_{\rm eff}$ is valid in the limit of $g\to 0$ or $M_W\to 0$. v is the vacuum expectation value, m_H is the Higgs-boson mass, and the W-boson mass $M_W=gv/2$. δ is zero at tree level and gets renormalized at the loop level. The small CP-violation effects from the Cabibbo-Kobayashi-Maskawa mixing angles in the SM are ignored in this work.

Because the leading contributions arise from the rescattering processes in (2.8), we only have to consider the longitudinally polarized $W^\pm$ and Z^0 in the first three processes listed in (2.6) for the initial-state scattering. Namely, we have to calculate

$$\begin{aligned} &e^-e^+\to W_L^-W_L^+\ ,\\ &e^-e^+\to Z_L^0Z_L^0\ ,\\ &e^-e^+\to Z_L^0H\ ,\\ &e^-e^+\to t\bar{t}\ ,\\ &e^-e^+\to b\bar{b}\ , \end{aligned} \tag{2.11}$$

in the high-energy limit, which is the limit that the energy of the W boson, E_W, is much bigger than M_W for a longitudinally polarized W boson W_L. (Here W can be either $W^\pm$ or Z^0.) Based on the ET, we can obtain the leading contributions of the first three processes listed in (2.11) by considering the equivalent processes

$$\begin{aligned} &e^-e^+\to\phi^-\phi^+\ ,\\ &e^-e^+\to\phi^0\phi^0\ ,\\ &e^-e^+\to\phi^0H\ . \end{aligned} \tag{2.12}$$

We note that the interaction Lagrangian used in calculating the amplitudes of these processes is the standard-model Lagrangian in R_ξ gauge, not the effective Lagrangian given in (2.10). In (2.12) the amplitude of the second process vanishes at the tree level if the mass of the electron is taken to be zero. As pointed out earlier, the third process cannot happen if the Higgs boson is too heavy to be produced on shell. Therefore, it will not contribute to the imaginary part of the scattering amplitudes. When the Higgs boson is light, we assume that m_H is of the order of M_W so that E_W is always bigger than M_W in the center-of-mass frame of e^-e^+, and the equivalence between the third process in (2.11) and that in (2.12) holds. But the amplitude of the third process in (2.12) vanishes at the tree level for a massless electron. Therefore, here-

after we shall not consider the contributions from either the $\phi^0\phi^0$ or $\phi^0 H$ intermediate state. We note that all the terms which are of $O(M_W/E_W)$ smaller than the leading contributions will be ignored in our calculation.

Following the procedures discussed above, we find that in the limit of taking the electron mass to be zero the only nonvanishing *equivalent* diagram corresponding to those shown in Fig. 3 is the triangle diagram shown in Fig. 4. The contribution from the self-energy diagram, as shown in Fig. 5, vanishes because it is always proportional to the momentum of the gauge boson which couples to massless fermions. The box diagram also vanishes because the coupling of the Goldstone boson with $e^{\pm}$ is proportional to the electron mass. Hence we only need to consider the contributions from the four triangle diagrams shown in Fig. 6 to obtain the degree of transverse polarization of the standard-model top quark produced via the process (1.1).

III. QCD CORRECTIONS

The degree of transverse polarization of the top quark arising from the QCD corrections for the process

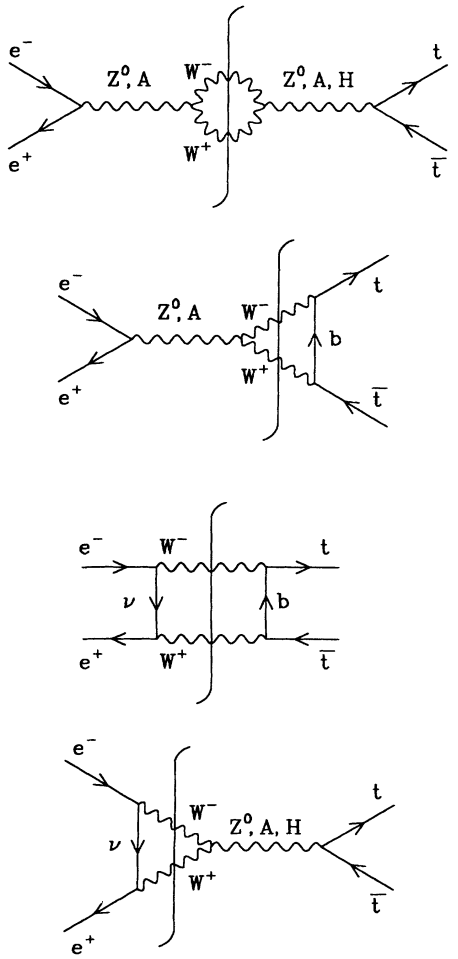

FIG. 3. Some of the diagrams contained in the first diagram of Fig. 2.

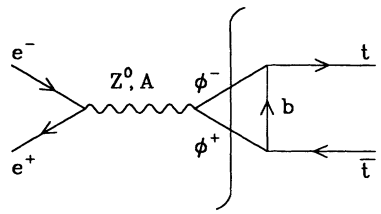

FIG. 4. Triangle diagram.

$e^-e^+ \to t\bar{t}$ has been discussed in Ref. [1]. We follow the notations used in that reference and present our results in terms of those form factors A, B, C, and D defined in Eq. (6.4) of Ref. [1]. The V-t-$\bar{t}$ vertex then takes the form

$$\Gamma^{\mu}_{Vtt} = ig\left[\gamma^{\mu}(F_1^L P_- + F_1^R P_+) - \frac{i\sigma^{\mu\nu}k_{\nu}}{m_t}(F_2^L P_- + F_2^R P_+)\right]$$
$$= \frac{ig}{2}\left[\gamma^{\mu}(A - B\gamma^5) + \frac{t_1^{\mu} - t_2^{\mu}}{2}(C - D\gamma^5)\right], \qquad (3.1)$$

where k^{μ} is the momentum of the gauge boson V and is taken by convention to be directed into the vertex. V can be the Z^0 gauge boson or photon A, and the F's are the form factors for V. In Eq. (3.1), $P_{\pm} = \frac{1}{2}(1 \pm \gamma_5)$, and t_1^{μ} (t_2^{μ}) is the momentum of the outgoing t ($\bar{t}$). In Ref. [1] we have given the helicity amplitudes of the process (1.1) in terms of these form factors; hence, we shall not repeat them here.

At tree level these form factors are real because the tree amplitudes are real, and

$$\mathrm{Re}(A) = 2v_t\ , \quad \mathrm{Re}(B) = 2a_t\ ,$$
$$\mathrm{Re}(C) = 0\ , \quad \mathrm{Re}(D) = 0\ , \qquad (3.2)$$

with

$$v_t = \frac{1}{4\cos\theta_W}[1 - \tfrac{8}{3}\sin^2\theta_W]\ , \quad \text{and}$$
$$a_t = \frac{1}{4\cos\theta_W} \quad \text{for } V = Z^0\ ; \qquad (3.3)$$
$$v_t = \tfrac{2}{3}\sin\theta_W\ , \quad a_t = 0 \quad \text{for } V = A\ .$$

θ_W is the weak mixing angle. At the one-loop level, the QCD corrections to these form factors can be obtained by calculating the diagram shown in Fig. 7. Since we are interested in the $O(\alpha_s)$ contribution to the transverse po-

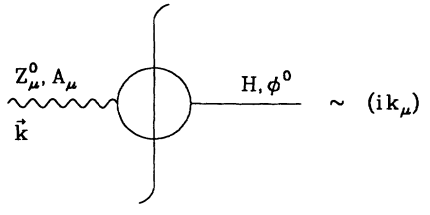

FIG. 5. Self-energy diagram.

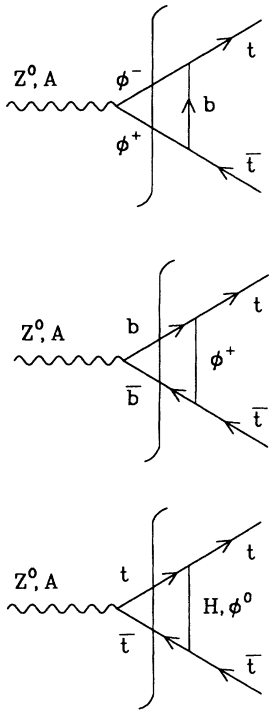

FIG. 6. Standard-model electroweak corrections.

larization of the top quark, we only consider the imaginary part of these form factors. They are

$$\mathrm{Im}(A)=v_t\frac{\alpha_s}{4\pi}(I_\infty-6\pi\beta)\ ,$$

$$\mathrm{Im}(B)=a_t\frac{\alpha_s}{4\pi}\left[I_\infty-\frac{2\pi}{\beta}(2+\beta^2)\right]\ , \tag{3.4}$$

$$\mathrm{Im}(C)=v_t\frac{\alpha_s}{4\pi}\left[\frac{-8\pi m_t}{S\beta}\right]\ ,\quad \mathrm{Im}(D)=0\ ,$$

where

$$\beta=\left[1-\frac{4m_t^2}{S}\right]^{1/2}\quad\text{and}\quad S=4E^2\ . \tag{3.5}$$

E is the energy of the top quark in the center-of-mass frame of $t\bar{t}$. I_∞ is not infrared finite and will not appear [2] in any physical observable, e.g., the degree of transverse polarization of the top quark. If we regularize this infrared singularity by a gluon mass m_g, then

$$I_\infty=\frac{2\pi(1+\beta^2)}{\beta}\ln\left[\frac{S\beta^2+m_g^2}{m_g^2}\right]\ . \tag{3.6}$$

$\mathrm{Im}(D)=0$ is due to the fact that QCD is a CP-invariant theory [1].

Given these form factors, we can calculate the degree of polarization, $P_\perp\sin\alpha$, of the top quark using the formulas listed in Ref. [1]. In Fig. 8 we show the distribution of $P_\perp\sin\alpha$ as a function of the top-quark polar angle θ_t in the center-of-mass frame of $t\bar{t}$ for various m_t and $\sqrt{S}$. They are of the order of a few percent. The leading contributions, obtained from the Born process, to the degree of the longitudinal polarization ($P_\parallel$), and the degree of the other transverse polarization ($P_\perp\cos\alpha$) of the top quark produced via the process (1.1) at the NLC can be found in Fig. 10 of Ref. [1]. In Fig. 9 of that reference, the θ_t distribution in the center-of-mass frame of $t\bar{t}$ was also given. The Born cross section of the process (1.1) for a 140-GeV top quark is 0.64 pb at $\sqrt{S}=0.5$ TeV and 0.18 pb at 1 TeV. For a 200-GeV top quark, the cross section is 0.49 pb at $\sqrt{S}=0.5$ TeV and 0.17 pb at 1 TeV. The strategy of testing the predictions of these polarizations can be found in Ref. [1] and the references therein.

IV. STANDARD-MODEL ELECTROWEAK CORRECTIONS

As discussed in Sec. II, only four triangle diagrams, shown in Fig. 6, need to be considered to obtain the transverse polarization of the top quark produced via the process (1.1) if the center-of-mass energy of e^-e^+ is large enough so that the calculation of using the ET is valid. We first express the loop integral in terms of the standard three-point form factors [10], reduce them to the stan-

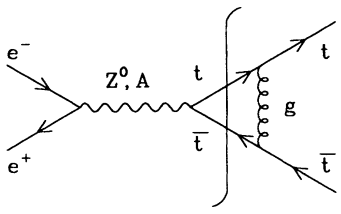

FIG. 7. QCD corrections.

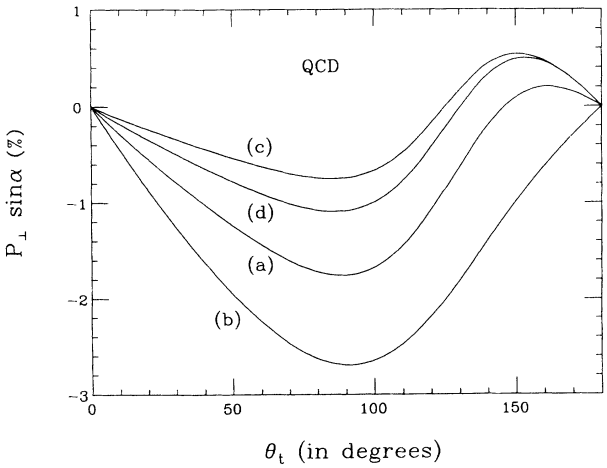

FIG. 8. $P_\perp\sin\alpha$, arising from the QCD corrections, as a function of the top-quark polar angle θ_t in the center-of-mass frame of $t\bar{t}$ for (a) $\sqrt{S}=0.5$ TeV, $m_t=140$ GeV; (b) $\sqrt{S}=0.5$ TeV, $m_t=200$ GeV; (c) $\sqrt{S}=1$ TeV, $m_t=140$ GeV; (d) $\sqrt{S}=1$ TeV, $m_t=200$ GeV.

dard scalar form factors [11], then apply the on-shell condition for t and $\bar{t}$, and identify the terms which correspond to the cutting diagrams. The leading corrections, which are of $O(m_t^2/v^2)$, to the imaginary part of those form factors A, B, C, and D, as defined in (3.1), are summarized as follows. We use the subscripts b, ϕ^+, ϕ^0, and H to indicate the contribution from the first, second, and third diagrams shown in Fig. 6.

From the first diagram of Fig. 6, we obtain

$$\begin{aligned}
&\mathrm{Im}(A_b)=f^V\frac{\alpha_t}{4\pi}\frac{\pi}{2\beta^2}\left[1+\beta^2-\frac{1}{2\beta}(1-2\beta^2+\beta^4)\times\ln\left[\frac{1+\beta}{1-\beta}\right]\right],\\
&\mathrm{Im}(B_b)=-\mathrm{Im}(A_b),\\
&\mathrm{Im}(C_b)=f^V\frac{\alpha_t}{4\pi}\frac{2\pi m_t}{S\beta^4}\left[3-\beta^2-\frac{1}{2\beta}(3-2\beta^2-\beta^4)\times\ln\left[\frac{1+\beta}{1-\beta}\right]\right],\\
&\mathrm{Im}(D_b)=0,
\end{aligned}\tag{4.1}$$

where

$$\begin{aligned}
&\alpha_t=\frac{1}{4\pi}\frac{m_t^2}{v^2},\\
&\beta=\left[1-\frac{4m_t^2}{S}\right]^{1/2},\\
&f^Z=\frac{1}{2\cos\theta_W}(\cos^2\theta_W-\sin^2\theta_W)\ \text{ for } V=Z^0,\\
&f^A=\sin\theta_W\ \text{ for } V=A.
\end{aligned}\tag{4.2}$$

We note that the validity of the ET does not require $\sin\theta_W=0$ for the processes listed in (2.11) and (2.12). One example is given in the Appendix.

Similarly, we obtain

$$\begin{aligned}
&\mathrm{Im}(A_{\phi^+})=(-v_b-a_b)\frac{\alpha_t}{4\pi}\frac{\pi}{2\beta^2}\left[1-3\beta^2-\frac{1}{2\beta}(1+2\beta^2-3\beta^4)\ln\left[\frac{1+\beta}{1-\beta}\right]\right],\\
&\mathrm{Im}(B_{\phi^+})=(-v_b-a_b)\frac{\alpha_t}{4\pi}\frac{\pi}{2\beta^2}\left[3-\beta^2-\frac{1}{2\beta}(3-2\beta^2-\beta^4)\ln\left[\frac{1+\beta}{1-\beta}\right]\right],\\
&\mathrm{Im}(C_{\phi^+})=(-v_b-a_b)\frac{\alpha_t}{4\pi}\frac{2\pi m_t}{S\beta^4}\left[3-\beta^2-\frac{1}{2\beta}(3-2\beta^2-\beta^4)\ln\left[\frac{1+\beta}{1-\beta}\right]\right],\\
&\mathrm{Im}(D_{\phi^+})=0,
\end{aligned}\tag{4.3}$$

where

$$\begin{aligned}
&v_b=\frac{1}{4\cos\theta_W}[-1+\tfrac{4}{3}\sin^2\theta_W],\quad a_b=\frac{-1}{4\cos\theta_W}\ \text{ for } V=Z^0;\\
&v_b=\frac{-1}{3}\sin\theta_W,\quad a_b=0\ \text{ for } V=A;
\end{aligned}\tag{4.4}$$

Also,

$$\begin{aligned}
&\mathrm{Im}(A_{\phi^0})=v_t\frac{\alpha_t}{4\pi}(\pi\beta),\\
&\mathrm{Im}(B_{\phi^0})=-a_t\frac{\alpha_t}{4\pi}(\pi\beta),\\
&\mathrm{Im}(C_{\phi^0})=v_t\frac{\alpha_t}{4\pi}\left[\frac{4\pi m_t}{S\beta}\right],\\
&\mathrm{Im}(D_{\phi^0})=0,
\end{aligned}\tag{4.5}$$

and

$$\mathrm{Im}(A_H)=v_t\frac{\alpha_t}{4\pi}\frac{\pi}{\beta}\left[\beta^2-\frac{2m_H^2}{S}+\frac{2}{\beta^2}\left[\frac{m_H^4}{S^2}+\beta^2-\beta^4\right]\ln\left[1+\frac{S\beta^2}{m_H^2}\right]\right],$$

$$\mathrm{Im}(B_H)=a_t\frac{\alpha_t}{4\pi}\frac{\pi}{\beta}\left\{3\beta^2-4+\frac{2m_H^2}{S}+\frac{2}{\beta^2}\left[(1-\beta^2)\left[\beta^2+\frac{2m_H^2}{S}\right]-\frac{m_H^4}{S^2}\right]\ln\left[1+\frac{S\beta^2}{m_H^2}\right]\right\},$$

$$\mathrm{Im}(C_H)=v_t\frac{\alpha_t}{4\pi}\frac{12\pi m_t}{S\beta}\left\{-1+\frac{2m_H^2}{S\beta^2}\left[-1+\left[1+\frac{m_H^2}{S\beta^2}\right]\ln\left[1+\frac{S\beta^2}{m_H^2}\right]\right]\right\}, \tag{4.6}$$

$$\mathrm{Im}(D_H)=0\ .$$

Note that $\mathrm{Im}(D)=0$ for all the diagrams shown in Fig. 6, becuase the standard model is a *CP*-invariant theory when we ignore the small *CP*-violation effects arising from the Cabibbo-Kobayashi-Maskawa mixing angles. Consequently, the degree of transverse polarization of t is the same in magnitude as that of $\bar{t}$ in the process (1.1), i.e.,

$$P_\perp\sin\alpha=-\bar{P}_\perp\sin\bar{\alpha}\ . \tag{4.7}$$

In Figs. 9 and 10, we show $P_\perp\sin\alpha$, due to the standard-model electroweak corrections, as a function of the top-quark polar angle θ_t in the center-of-mass frame of $t\bar{t}$ for various $\sqrt{S}$, m_t, and m_H. By comparing Figs. 8 and 9, we conclude that the degree of transverse polarization of the top quark arising from the SM electroweak corrections is smaller than that from the QCD corrections for a 140-GeV top quark produced via the process (1.1) at the NLC. But the SM electroweak corrections become more important than the QCD corrections when the top quark becomes heavier ($m_t=200$ GeV) at $\sqrt{S}=1$ TeV. The contribution to the transverse polarization of the top quark due to the Higgs-boson-exchange interaction, as shown in Fig. 6, can be estimated by the difference in $P_\perp\sin\alpha$ between a theory with a 100-GeV Higgs boson and the other with a 1-TeV Higgs boson. From Figs. 9 and 10, we find that the contribution of the Higgs-boson-exchange interaction is small; it is typically of the order of a percent. Hence it requires that the degree of transverse polarization of the top quark be measured better than a percent level in order to probe the Higgs boson by this measurement. The strategies of measuring the polarization of the top quark were discussed in Ref. [1]; we shall not repeat them here.

V. NONSTANDARD ELECTROWEAK CORRECTIONS

A. Electroweak theory with dynamical symmetry breaking

In the SM, fermions are coupled via Yukawa interactions to the Higgs doublet and acquire masses when the Higgs field acquires a nonzero vacuum expectation value. In general, this is not the case in an electroweak theory with dynamical symmetry breaking. It was shown in Ref. [5] that there exist some *nonuniversal* gauge interactions when considering a coset space G/H with $G=\mathrm{SU}(2)_L\times\mathrm{U}(1)_Y$ and $H=\mathrm{U}(1)_{\mathrm{em}}$. In this section we study the top-quark polarization predicted by the theory proposed

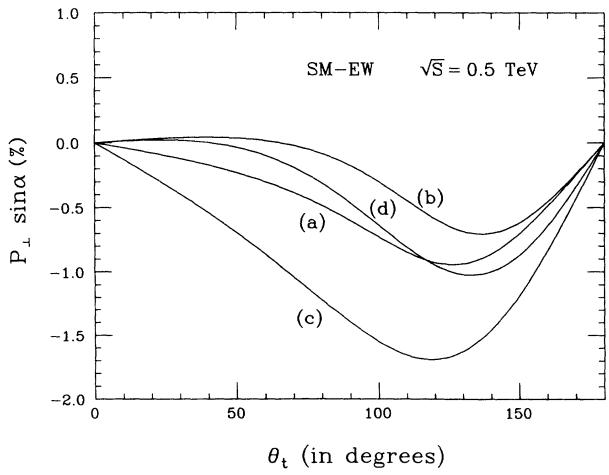

FIG. 9. $P_\perp\sin\alpha$, arising from the standard-model electroweak corrections, as a function of θ_t in the center-of-mass frame of $t\bar{t}$ for (a) $m_t=140$ GeV, and $m_H=0.1$ TeV; (b) $m_t=140$ GeV, $m_H=1$ TeV; (c) $m_t=200$ GeV, $m_H=0.1$ TeV; (d) $m_t=200$ GeV, $m_H=1$ TeV; at $\sqrt{S}=0.5$ TeV.

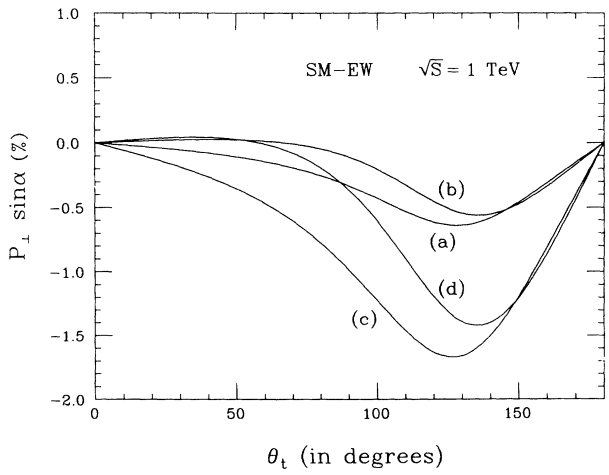

FIG. 10. $P_\perp\sin\alpha$, arising from the standard-model electroweak corrections, as a function of θ_t in the center-of-mass frame of $t\bar{t}$ for (a) $m_t=140$ GeV, $m_H=0.1$ TeV; (b) $m_t=140$ GeV, $m_H=1$ TeV; (c) $m_t=200$ GeV, $m_H=0.1$ TeV; (d) $m_t=200$ GeV, $m_H=1$ TeV; at $\sqrt{S}=1$ TeV.

in that reference.

We assume that the interactions of the leptons and light quarks (u,d,s,c) are standard, and well described by the SM model. However, the interactions of the heavy quarks (b,t) are described by the chiral Lagrangian given in Ref. [5]. The relevant chiral Lagrangian (CL) for our study is

$$\mathcal{L}_{\rm CL}=\mathcal{L}_0+\mathcal{L}_1 , \tag{5.1}$$

with

$$\begin{aligned}\mathcal{L}_0&=\overline{\Psi_L}(i\not{D})\Psi_L+\overline{\Psi_R}(i\not{D})\Psi_R-\overline{\Psi_L}\Sigma M\Psi_R-\overline{\Psi_R}M^\dagger\Sigma^\dagger\Psi_L+\tfrac{1}{2}v_a^2\Sigma_{a\mu}\Sigma_a^\mu ,\\ \mathcal{L}_1&=-\overline{\Psi_L}\Sigma\gamma_\mu(\kappa_L^{\rm NC})\Sigma^\dagger\Psi_L\Sigma_3^\mu-\overline{\Psi_R}\gamma_\mu(\kappa_R^{\rm NC})\Psi_R\Sigma_3^\mu-\sqrt{2}\overline{\Psi_L}\Sigma\gamma_\mu\tau_+(\kappa_L^{\rm CC})\Sigma^\dagger\Psi_L\Sigma_+^\mu\\ &\quad-\sqrt{2}\overline{\Psi_L}\Sigma\gamma_\mu\tau_-(\kappa_L^{\rm CC})^\dagger\Sigma^\dagger\Psi_L\Sigma_-^\mu-\sqrt{2}\overline{\Psi_R}\gamma_\mu\tau_+(\kappa_R^{\rm CC})\Psi_R\Sigma_+^\mu-\sqrt{2}\overline{\Psi}_R\gamma_\mu\tau_-(\kappa_R^{\rm CC})^\dagger\Psi_R\Sigma_-^\mu ,\end{aligned} \tag{5.2}$$

where

$$\begin{aligned}&\Sigma=\exp\left[i\frac{\tau_a\phi_a}{v_a}\right] , \quad a=1,2,3 ,\\ &\Sigma_{a\mu}=\frac{-i}{2}{\rm Tr}(\tau_a\Sigma^\dagger D_\mu\Sigma) ,\\ &\Psi_L=\begin{bmatrix}t\\b\end{bmatrix}_L , \quad \Psi_R=\begin{bmatrix}t\\b\end{bmatrix}_R ,\\ &\tau_+=\begin{bmatrix}0&1\\0&0\end{bmatrix} , \quad \tau_-=\begin{bmatrix}0&0\\1&0\end{bmatrix} ,\\ &M=\begin{bmatrix}m_t&0\\0&m_b\end{bmatrix} ,\\ &D_\mu\Psi_L=\left[\partial_\mu-ig\frac{\tau_a}{2}W_{a\mu}-ig'\tfrac{1}{6}Y_\mu\right]\Psi_L ,\\ &D_\mu\Psi_R=(\partial_\mu-ig'y_R Y_\mu)\Psi_R ,\\ &D_\mu\Sigma=\partial_u\Sigma-ig\frac{\tau_a}{2}W_{a\mu}\Sigma+ig'\Sigma\frac{\tau_3}{2}Y_\mu .\end{aligned} \tag{5.3}$$

ϕ_a are the Goldstone-boson fields. τ_a are the Pauli matrices. Since the $U(1)_{\rm em}$ symmetry is preserved, the vacuum expectation values $v_1=v_2=v$. But v_3 in general does not have to be equal to v if there is no additional SU(2) custodial symmetry in the theory. Ψ_R is an $SU(2)_L$ singlet. M is the quark-mass matrix. y_R is the right-handed quark charge, being $\frac{2}{3}$ for t and $-\frac{1}{3}$ for b. The fields W_3 and Y are related to Z^0 and A via

$$\begin{bmatrix}W_3\\Y\end{bmatrix}=\begin{bmatrix}\cos\theta_W&\sin\theta_W\\-\sin\theta_W&\cos\theta_W\end{bmatrix}\begin{bmatrix}Z^0\\A\end{bmatrix} \quad \text{with } \tan\theta_W=\frac{g'}{g} . \tag{5.4}$$

If $v_3=v$, then in the unitary gauge, corresponding to $\Sigma=1$, the locally $SU(2)_L\times U(1)_Y$-invariant Lagrangian obtained from $\mathcal{L}_0$ is that of the SM in the limit of $m_H\to\infty$. The nonuniversal interactions of the heavy quarks are described by the parameters $\kappa_{L,R}^{\rm NC}$ and $\kappa_{L,R}^{\rm CC}$. Based on the Hermiticity of the interaction Lagrangian, $\kappa_{L,R}^{\rm NC}$ have to be real. But $\kappa_{L,R}^{\rm CC}$ in general can be complex. (We note that $\kappa_{L,R}^{\rm NC}$ and $\kappa_{L,R}^{\rm CC}$ in general can be matrices in flavor space [5].)

In order to obtain an effective Lagrangian, similar to the one given in (2.10) for the SM, for this theory in the high-energy limit, we expand $\mathcal{L}_{\rm CL}$ in ϕ_a and keep the first relevant terms with the fermion and/or Goldstone-boson fields. Define

$$\phi^\pm=\frac{1}{\sqrt{2}}(\phi_1\mp i\phi_2) . \tag{5.5}$$

We obtain

$$\begin{aligned}\mathcal{L}_0\to&\,\bar t(i\not{\partial}-m_t)t+\bar b(i\not{\partial}-m_b)b+(\partial_\mu\phi^+)(\partial^\mu\phi^-)\\ &+\tfrac{1}{2}(\partial_\mu\phi^0)^2-\frac{im_t}{\sqrt{2}v}\phi^-\bar b(1+\gamma_5)t\\ &+\frac{im_t}{\sqrt{2}v}\phi^+\bar t(1-\gamma_5)b-\frac{im_t}{v_3}\phi^0\bar t\gamma_5 t\\ &+\frac{im_b}{\sqrt{2}v}\phi^-\bar b(1-\gamma_5)t-\frac{im_b}{\sqrt{2}v}\phi^+\bar t(1+\gamma_5)b\\ &+\frac{im_b}{v_3}\phi^0\bar b\gamma_5 b ,\\ \mathcal{L}_1\to&-\frac{1}{\sqrt{2}v}(\partial^\mu\phi^-)\bar b\gamma_\mu[\kappa_L^{\rm CC}(1-\gamma_5)+\kappa_R^{\rm CC}(1+\gamma_5)]t\\ &-\frac{1}{\sqrt{2}v}(\partial^\mu\phi^+)\bar t\gamma_\mu[\kappa_L^{\rm CC\dagger}(1-\gamma_5)+\kappa_R^{\rm CC\dagger}(1+\gamma_5)]b\\ &-\frac{1}{2v_3}(\partial^\mu\phi^0)\bar t\gamma_\mu[\kappa_L^{\rm NC}(1-\gamma_5)+\kappa_R^{\rm NC}(1+\gamma_5)]t .\end{aligned} \tag{5.6}$$

The nonuniversal gauge couplings can be obtained from $\mathcal{L}_1$ in (5.2) in the unitary gauge $\Sigma=1$. The relevant interaction Lagrangian is

$$\begin{aligned}&\frac{g}{2\sqrt{2}}W_\mu^+\bar t\gamma^\mu[(\kappa_L^{\rm CC}+\kappa_R^{\rm CC})-\gamma_5(\kappa_L^{\rm CC}-\kappa_R^{\rm CC})]b+{\rm H.c.}\\ &\quad+\frac{g}{4\cos\theta_W}Z_\mu^0\bar t\gamma^\mu[(\kappa_L^{\rm NC}+\kappa_R^{\rm NC})-\gamma_5(\kappa_L^{\rm NC}-\kappa_R^{\rm NC})]t ,\end{aligned} \tag{5.7}$$

which should be compared with the standard couplings, obtained from $\mathcal{L}_0$ in (5.2):

$$\begin{aligned}&\frac{g}{2\sqrt{2}}W_\mu^+\bar t\gamma^\mu(1-\gamma_5)b+{\rm H.c.}\\ &\quad+\frac{g}{4\cos\theta_W}Z_\mu^0\bar t\gamma^\mu\left[\left(1-\frac{8}{3}\sin^2\theta_W\right)-\gamma_5\right]t .\end{aligned} \tag{5.8}$$

Hereafter, we shall take $m_b=0$ and follow the assumption made in Ref. [12] that $\kappa_{L,R}^{CC}$ is negligible compared with $\kappa_{L,R}^{NC}$.

B. Top-quark polarization in the chiral Lagrangian theory

We shall consider the polarization of the top quark produced via the process (1.1) in the chiral Lagrangian theory discussed in Sec. V A.

For simplicity, we follow the assumption made in Ref. [12] and take $m_b=0$, $v_3=v$, $\kappa_L^{CC}=\kappa_R^{CC}=0$, and $\kappa_L^{NC}=\kappa_R^{NC}=\kappa^{NC}$. (We have used the result obtained in Ref. [12] that the current experimental bounds on these nonstandard couplings are such that κ_L^{NC} is about equal to κ_R^{NC}.) Under this assumption there is only one extra free parameter κ^{NC} in this theory compared with the SM. The nonstandard Z^0-t-$\bar{t}$ coupling is purely vectorlike. We note that in this theory there is no Higgs-boson field; therefore, the triangle diagram, as shown in Fig. 6, with the Higgs boson being one of the internal lines does not exist in this theory. The standard contributions to the degree of transverse polarization of the top quark in this theory can be obtained from the diagrams shown in Fig. 6. But the Higgs-boson-exchange diagram should not be included. There are also some nonstandard contributions arising from the nonstandard couplings of Z^0-t-$\bar{t}$ and ϕ^0-t-$\bar{t}$, as described by Eqs. (5.6) and (5.7), in this theory. Again, we follow the assumption made in Ref. [12] that only the corrections linear in κ^{NC}, i.e., terms of $O((\alpha_t/4\pi)\kappa^{NC})$, are kept when we consider the non-standard contributions in calculating $P_\perp \sin\alpha$ of the top quark. The Feynman diagrams to be considered are those shown in Fig. 11. The standard contributions to the form factors A, B, C, and D in this theory can then be obtained from (4.1), (4.3), and (4.5). The nonstandard contributions from the sum of the second and third diagrams in Fig. 11 vanish. The first diagram in Fig. 11 gives

$$\begin{aligned}
&\mathrm{Im}(A_{\phi^0}^{NS})=v_t^{NS}\frac{\alpha_t}{4\pi}(\pi\beta)\ ,\\
&\mathrm{Im}(B_{\phi^0}^{NS})=-a_t^{NS}\frac{\alpha_t}{4\pi}(\pi\beta)\ ,\\
&\mathrm{Im}(C_{\phi^0}^{NS})=v_t^{NS}\frac{\alpha_t}{4\pi}\left[\frac{4\pi m_t}{S\beta}\right]\ ,\\
&\mathrm{Im}(D_{\phi^0}^{NS})=0\ ,
\end{aligned}\tag{5.9}$$

where

$$\begin{aligned}
v_t^{NS}&=\frac{1}{4\cos\theta_W}(\kappa_L^{NC}+\kappa_R^{NC})=\frac{1}{2\cos\theta_W}\kappa^{NC}\ ,\\
a_t^{NS}&=\frac{1}{4\cos\theta_W}(\kappa_L^{NC}-\kappa_R^{NC})=0\ .
\end{aligned}\tag{5.10}$$

In Fig. 12 we show $P_\perp \sin\alpha$ predicted by this theory as a function of the top-quark polar angle θ_t in the center-of-mass frame of $t\bar{t}$ for various κ^{NC} with $m_t=200$ GeV at $\sqrt{S}=1$ TeV. We show the results for $\kappa^{NC}=-1,0,1$. (The upper bound on κ^{NC} as a function of m_t and the cutoff scale of the theory can be found in Ref. [12].) We also show the SM prediction with $m_H=1$ TeV in Fig. 12 for comparison. The difference between the curves (e) and (a) in Fig. 12 is due to the contribution from the 1-TeV Higgs-boson-exchange diagram in the SM. Again,

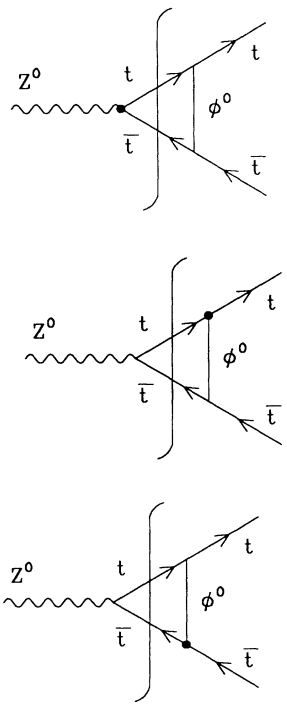

FIG. 11. Nonstandard contributions to $P_\perp \sin\alpha$. The vertex with dot indicates nonstandard coupling.

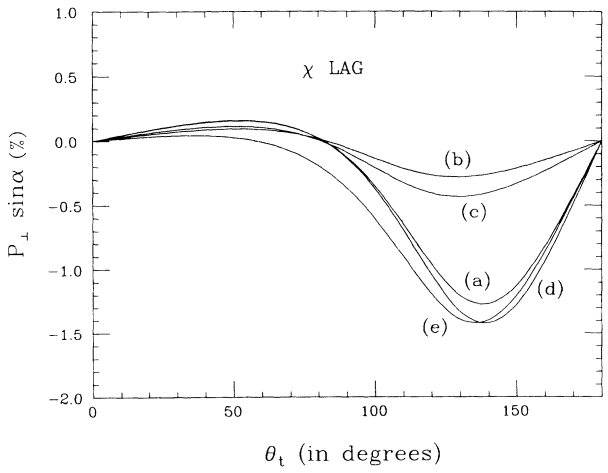

FIG. 12. $P_\perp \sin\alpha$ as a function of the top-quark polar angle θ_t in the center-of-mass frame of $t\bar{t}$ for (a) $\kappa^{NC}=0$, (b) $\kappa^{NC}=1$, (c) $\kappa^{NC}=-1$, and (d) $\kappa^{NC}=-0.2$ in the theory with dynamical symmetry breaking, and (e) in the SM with $m_H=1$ TeV. We take $m_t=200$ GeV and $\sqrt{S}=1$ TeV.

we see that the SM Higgs-boson contribution to the transverse polarization $P_\perp \sin\alpha$ is small. For completeness, we also show in Fig. 13 the leading contributions to the degree of the longitudinal polarization $P_\parallel$ and the degree of the other transverse polarization $P_\perp \cos\alpha$ of the top quark produced via the process (1.1). In Fig. 13 only the Born process is considered. The coupling of A-t-$\bar{t}$ is standard, and the coupling of Z^0-t-$\bar{t}$ contains both the standard and nonstandard pieces. We find that both $P_\parallel$ and $P_\perp \cos\alpha$ are sensitive to $\kappa^{\rm NC}$. To explore this point, we show in Fig. 14 the distributions of $P_\parallel$ and $P_\perp \cos\alpha$ as a function of $\kappa^{\rm NC}$ for a fixed θ_t in the center-of-mass frame of $t\bar{t}$. We therefore conclude that a TeV e^-e^+ collider will be extremely useful to test the coupling of Z^0-t-$\bar{t}$. θ_t distribution of the top quark at tree level for various $\kappa^{\rm NC}$ in the center-of-mass frame of $t\bar{t}$ is shown in Fig. 15. The Born cross section of the process (1.1) in this theory for a 200-GeV top quark is 0.17 pb for $\kappa^{\rm NC}=0$, 0.40 pb for $\kappa^{\rm NC}=1$, and 0.24 pb for $\kappa^{\rm NC}=-1$ at $\sqrt{S}=1$ TeV. The cross section for $\kappa^{\rm NC}=0$ in this theory is the same as that predicted by the SM. Similarly, the

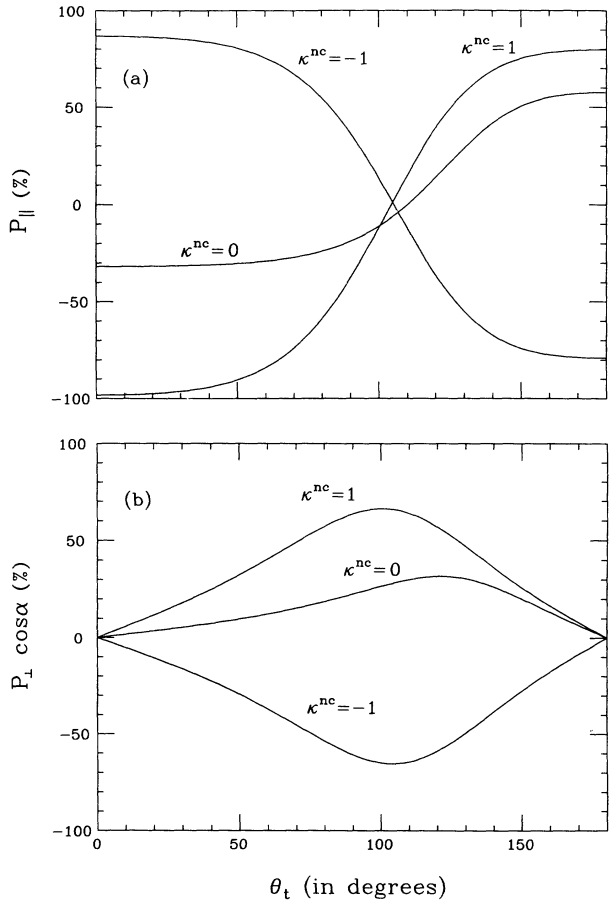

FIG. 13. (a) $F_\parallel$ and (b) $P_\perp \cos\alpha$ distributions of the top quark produced via $e^-e^+ \to t\bar{t}$ in the theory with dynamical symmetry breaking for various $\kappa^{\rm NC}$ at $\sqrt{S}=1$ TeV. m_t is taken to be 200 GeV.

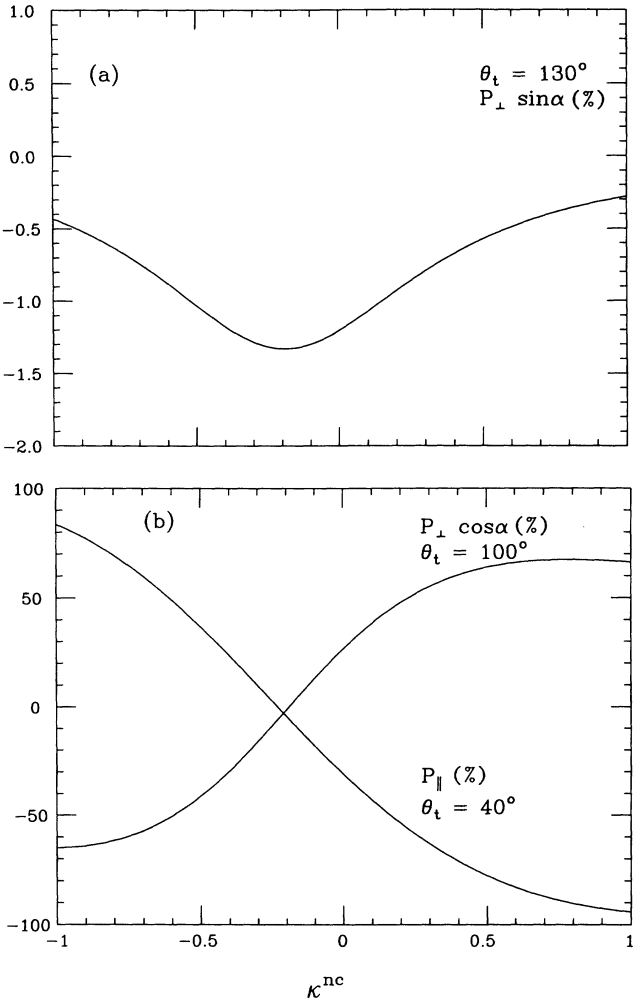

FIG. 14. (a) $P_\perp \sin\alpha$ and (b) $P_\parallel$ and $P_\perp \cos\alpha$ distributions as a function of $\kappa^{\rm NC}$ for a fixed θ_t in the center-of-mass frame of $t\bar{t}$. $\sqrt{S}=1$ TeV and $m_t=200$ GeV.

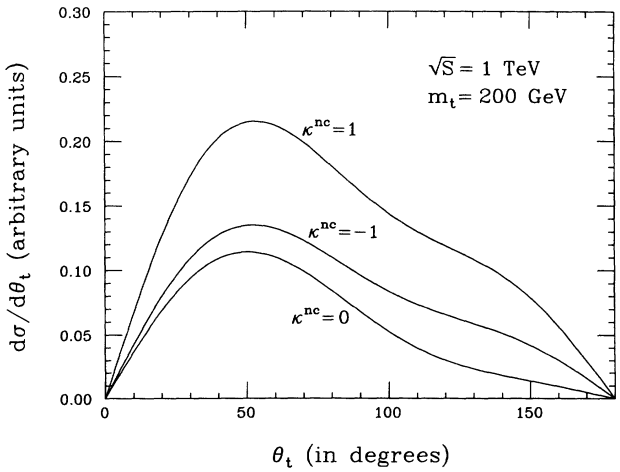

FIG. 15. θ_t distribution of the top quark at tree level in the center-of-mass frame of $t\bar{t}$ for various $\kappa^{\rm NC}$ with $m_t=200$ GeV and $\sqrt{S}=1$ TeV.

coupling of W-t-b can be studied via the tree-level photon-W fusion process [1]

$$e^-e^+ \to \gamma W \to e^- \bar{\nu}_e t\bar{b} \quad \text{or} \quad e^+\nu_e \bar{t} b \ . \tag{5.11}$$

VI. DISCUSSIONS AND CONCLUSIONS

As discussed in Ref. [1], measuring the polarization of the top quark produced via process (1.1) provides a method to test the gauge coupling V-t-$\bar{t}$. The coupling of W-t-b can be tested by the polarization of the W boson from the decay of the top quark or by studying the photon-W fusion process (5.11). The strategies of measuring the polarization of t and W were discussed in our previous work [1]. Here we showed the degree of polarization of the top quark predicted by the QCD, the standard model electroweak theory, and an electroweak theory with dynamical symmetry breaking [5]. For the transverse polarization $P_\perp \sin\alpha$ of the top quark, we considered the radiative corrections of $O(\alpha_s)$ for QCD, $O(m_t^2/v^2)$ for SM, and $O(m_t^2/v^2, (m_t^2/v^2)\kappa^{\rm NC})$ for the chiral Lagrangian. The calculation of obtaining the electroweak corrections was simplified by applying the equivalence theorem. As for the longitudinal polarization $P_\parallel$ and the other transverse polarization $P_\perp \cos\alpha$ of the top quark, we considered the Born process to calculate the leading contributions in various theories.

We found that at the NLC the contribution to the transverse polarization of the top quark arising from a loop due to the electroweak exchange rather than the gluon exchange is less than the QCD contribution for m_t of about 140 GeV. This includes Higgs-boson exchange, whose effect in magnitude is less than 1%. We also examined the polarization of the top quark arising from an electroweak theory [5] with dynamical symmetry breaking and conclude that the polarization of the top quark is sensitive to $\kappa^{\rm NC}$, which is used to parametrize the nonuniversal gauge coupling of Z^0-t-$\bar{t}$. In this work we used the result given in Ref. [5] and assumed that only the vector part of the Z^0-t-$\bar{t}$ vertex has nonstandard contributions.

In addition to the polarization of the top quark, we also pointed out the importance of testing the CP property of a theory in Ref. [1]. The strategies of testing the CP prediction of a theory were also discussed in that reference. QCD is a CP-invariant theory. The CP-violation effects in the standard model that arise from the Cabibbo-Kobayashi-Maskawa mixing angles are small. The electroweak theory with dynamical symmetry breaking considered in this paper can in principle have large CP-violation effects arising from the complex matrices $(\kappa_{L,R}^{\rm CC})_{ij}$, which parametrize the nonuniversal gauge coupling of W-t-b. The subscripts i and j are the family indices. If Im(D) does not vanish when considering a theory with nonzero complex $(\kappa_{L,R}^{\rm CC})_{ij}$, then the degree of transverse polarization of the top antiquark will be different in magnitude from that of the top quark produced via (1.1), and the theory is CP violating. In this paper we follow the assumption made in Ref. [12] and only consider a CP-invariant theory. It is interesting to know what the current experimental bounds on these nonstandard couplings $(\kappa_{L,R}^{\rm CC})_{ij}$ are, and what the prediction of this theory is in the CP-violation effects to appear in the top-quark physics either at e^-e^+ or hadron colliders. We shall leave this for a future study [13].

CP-violation effects from other kinds of interactions, e.g., a two-Higgs-doublet model, are currently studied by Peskin and Schmidt [14].

ACKNOWLEDGMENTS

I am grateful to G. L. Kane and G. A. Ladinsky for a pleasant collaboration on this study. I thank J. A. Bagger, E. L. Berger, M. Dine, H. Haber, M. Peskin, C. Schmidt, and R. Vega for discussions. I would also like to express my gratitude to the Texas National Research Laboratory Commission for financial support.

APPENDIX: VALIDITY OF THE EQUIVALENCE THEOREM

We give an example to demonstrate that the validity of the equivalence theorem does not require $\sin\theta_W$ to be zero, where θ_W is the weak mixing angle.

Let us consider the scattering process

$$e_+^- e_-^+ \to W_L^- W_L^+ \ , \tag{A1}$$

at the tree level. e_+^- denotes a right-handed e^-, W_L^- a longitudinal W^-. The helicity amplitude for this process is

$$A_W = \frac{16\sin^2\theta_W}{v^2}\left[\frac{1}{S-M_Z^2}-\frac{1}{S}\right](3E^3K - EK^3)\sin\theta \ , \tag{A2}$$

where $S=4E^2$, $K=(E^2-M_W^2)^{1/2}$, and θ is the angle between W^- and e^- in the center-of-mass frame of e^-e^+.

The helicity amplitude of the *equivalent* process

$$e_+^- e_-^+ \to \phi^-\phi^+ \ , \tag{A3}$$

in the high-energy limit $E > M_W$, is

$$A_\phi = \frac{16\sin^2\theta_W}{v^2}\left[\left[1-\frac{1}{2\cos^2\theta_W}\right]\frac{1}{S-M_Z^2}-\frac{1}{S}\right] \times (EKM_W^2)\sin\theta \ . \tag{A4}$$

In the high-energy limit $E > M_W$,

$$\frac{1}{S-M_Z^2} \simeq \frac{1}{S}\left[1+\frac{M_Z^2}{S}\right] \ , \quad K \simeq E\left[1-\frac{M_W^2}{2E^2}\right] \ . \tag{A5}$$

Using the tree-level relation between the Z^0 and $W^\pm$ masses,

$$M_Z = \frac{M_W}{\cos\theta_W} = \frac{gv}{2\cos\theta_W} \ , \tag{A6}$$

we obtain

$$A_\phi = (-i)^2 A_W = -\frac{g^2 \sin^2\theta_W}{2\cos^2\theta_W}\sin\theta \ , \tag{A7}$$

in the limit of $E > M_W, M_Z$.

Hence we have shown that in the high-energy limit the leading contributions of (A1) and (A3) are the same for all $\sin\theta_W$.

[1] G. L. Kane, G. A. Ladinsky, and C.-P. Yuan, Phys. Rev. D **45**, 124 (1992).

[2] G. L. Kane, J. Pumplin, and W. Repko, Phys. Rev. Lett. **41**, 1689 (1978); A. Devoto, G. L. Kane, J. Pumplin, and W. Repko, *ibid.* **43**, 1062 (1979); **43**, 1540 (1979); A. Devoto, G. L. Kane, J. Pumplin, and W. Repko, Phys. Lett. **90B**, 436 (1980).

[3] D. Sivers, Report No. ANL-HEP-PR-90-93, 1990 (unpublished).

[4] J. M. Cornwall, D. N. Levin, and G. Tiktopoulos, Phys. Rev. D **10**, 1145 (1974); C. Vayonakis, Lett. Nuovo Cimento **17**, 383 (1976); B. W. Lee, C. Quigg, and H. Thacker, Phys. Rev. D **16**, 1519 (1977); M. S. Chanowitz and M. K. Gaillard, Nucl. Phys. **B261**, 379 (1985); G. J. Gounaris, R. Kogerler, and H. Neufeld, Phys. Rev. D **34**, 3257 (1986); Y.-P. Yao and C.-P. Yuan, *ibid.* **38**, 2237 (1988); J. Bagger and C. Schmidt, *ibid.* **41**, 264 (1990); H. Veltman, *ibid.* **41**, 2294 (1990).

[5] R. D. Peccei and X. Zhang, Nucl. Phys. **B337**, 269 (1990).

[6] R. E. Cutkosky, J. Math. Phys. **1**, 429 (1960).

[7] C.-P. Yuan and T.-C. Yuan, Phys. Rev. D **44**, 3603 (1991).

[8] B. W. Lee, C. Quigg, and H. B. Thacker, Phys. Rev. Lett. **38**, 883 (1977); Phys. Rev. D **16**, 1519 (1977); M. S. Chanowitz, M. A. Furman, and I. Hinchliffe, Nucl. Phys. **B153**, 402 (1979).

[9] S. Dawson, G. Kane, C.-P. Yuan, and S. Willenbrock, in *Physics of the Superconducting Super Collider, Snowmass, 1986,* Proceedings of the Summer Study, Snowmass, Colorado, edited by R. Donaldson and J. Marx (Division of Particles and Fields of the APS, New York, 1987), p. 235; C.-P. Yuan, Nucl. Phys. **B310**, 1 (1988).

[10] G. Passarino and M. Veltman, Nucl. Phys. **B160**, 151 (1979).

[11] G. 't Hooft and M. Veltman, Nucl. Phys. **B153**, 365 (1979).

[12] R. D. Peccei, S. Peris, and X. Zhang, Nucl. Phys. **B349**, 305 (1991).

[13] C. Kao and C.-P. Yuan (unpublished).

[14] M. Peskin and C. Schmidt (private communication).